Geophysical Research Letters

RESEARCH LETTER

10.1029/2020GL088578

# The Contribution of Sprite Streamers to the Chemical Composition of the Mesosphere-Lower Thermosphere

F. J. Pérez-Invernón[1,2], A. Malagón-Romero[1], F. J. Gordillo-Vázquez[1], and A. Luque[1]

[1]Instituto de Astrofísica de Andalucía (IAA), CSIC, Granada, Spain, [2]Deutsches Zentrum für Luft- und Raumfahrt, Institut für Physik der Atmosphäre, Oberpfaffenhofen, Germany

**Key Points:**

- The injection of $N_2O$ by sprites seems to be not enough to account for the disagreement between satellite observations and simulations
- We have calculated the radial dependence of the production of NO and $N_2O$ by a single sprite streamer in the mesosphere
- The characteristics of the LBH band emitted by sprites prevent the estimation of the event altitude from space-based photometric recordings

**Correspondence to:**
F. J. Pérez-Invernón,
FranciscoJavier.Perez-Invernon@dlr.de

**Citation:**
Pérez-Invernón, F. J., Malagón-Romero, A., Gordillo-Vázquez, F. J., & Luque, A. (2020). The contribution of sprite streamers to the chemical composition of the mesosphere-lower thermosphere. *Geophysical Research Letters*, *47*, e2020GL088578. https://doi.org/10.1029/2020GL088578

Received 24 APR 2020
Accepted 17 JUN 2020
Accepted article online 20 JUN 2020



**Abstract** Sprites are mesospheric filamentary discharges that liberate and accelerate large quantities of electrons. They produce local enhancements of some chemical species and fast (millisecond) optical emissions. In this work, we couple a self-consistent 2-D model of sprites with an extensive chemical scheme to calculate the injection of chemical species by one sprite streamer in the mesosphere 0.85 ms after its onset. The N, NO, and $N_2O$ injections per streamer are about $10^{21}$ atoms, $6 \times 10^{19}$ molecules, and $10^{18}$ molecules, respectively. According to our results, longer simulations are necessary to determine the role of sprites in the concentration of $N_2O$ in the mesosphere. We also calculate the contribution of sprite glows to space-based photometers of the Atmosphere-Space Interactions Monitor and the Tool for the Analysis of RAdiations from lightNIngs and Sprites.

## 1. Introduction

Sprites are a type of transient luminous event (TLE) with a characteristic time of few milliseconds taking place in the range of altitudes between 40 and 90 km above thunderstorms (e.g., Franz et al., 1990; Pasko et al., 1997, 2012; Stenbaek-Nielsen et al., 3829). They are formed by fast-propagating bright plasma filaments known as streamers (Pasko et al., 1998; Raizer et al., 1998) followed by long-standing (1–100 ms) luminous structures called beads and glows (Liu, 2010; Luque & Gordillo-Vázquez, 2011; Luque et al., 2016).

Since their discovery in 1989, several authors have investigated the chemical influence of sprites in the mesosphere using zero- and one-dimensional models (e.g., Evtushenko et al., 2013; Gordillo-Vázquez, 2008, 2010, 2012; Parra-Rojas et al., 2015; Sentman et al., 2008; Winkler & Nothold, 2014). They reported a significant production of NO in the center of sprite streamers due to the oxidation of atomic nitrogen produced by electron-impact processes. Sentman et al. (2008) assumed a streamer nominal diameter of 25 m and a vertical length of 10 km to estimate a production of $5 \times 10^{19}$ molecules of NO per streamer between altitudes 65 and 75 km. In the stratosphere, $NO_x$ produced by lightning contributes to ozone depletion (Crutzen, 1979; Schumann & Huntrieser, 2007), while its concentration in the mesosphere is very low. Enell et al. (2008) estimated a production of $3 \times 10^{22}$–$3 \times 10^{23}$ molecules of NO per sprite. Arnone et al. (2014) used these estimated $NO_x$ production to calculate, using the Whole Atmosphere Community Climate Model version 4 (WACCM4), the global and regional sprite-induced variations in the concentration of $NO_x$. They found that the perturbation in the tropical concentration of nitrogen oxide by sprite streamers could lie between 0.015 and 0.15 ppbv. These quantities correspond to a perturbation of the background concentration of $NO_x$ between less than 1% and up to 20%. Rodger et al. (2008), Arnone et al. (2008), Arnone et al. (2009), and Arnone and Dinelli (2016) reported $NO_x$ over thunderstorms through satellite observations. They concluded that sprite-$NO_x$ is at the edge of detectability with current instruments.

The third strongest greenhouse gas after $CO_2$ and $CH_4$ is $N_2O$, having a global-warming potential (GWP) of almost 300 over 100 years and being an important ozone depleting species (Davidson, 2009). The most important source of $N_2O$ in the atmosphere is from surface emissions (Davidson, 2009). However, Sheese et al. (2016) reported the existence of an atmospheric source of $N_2O$ based on observations from the satellite instrument "Atmospheric Chemistry Experiment-Fourier Transform Spectrometer" (ACE-FTS). They proposed energetic particle precipitation in the lower thermosphere as the main $N_2O$ atmospheric source. Kelly et al. (2018) included the production of $N_2O$ via $N_2(A^3\Sigma_u^+) + O_2$ in the mesosphere-lower thermosphere (MLT) in

WACCM. Their results supported the $N_2O$ measurements provided by ACE-FTS. However, their simulations produced less $N_2O$ than observed between 60 and 80 km over middle and low latitudes.

Winkler and Nothold (2015) proposed Blue Jets, another type of TLE, as a possible source of $N_2O$ in the lower stratosphere. Based on results by Winkler and Nothold (2015), Pérez-Invernón et al. (2019) developed the first global parameterization for Blue Jets and implemented it in WACCM4. These authors reported that Blue Jets could contribute to about 38% of the $N_2O$ between 20 and 40 km. Previously, Gordillo-Vázquez (2008) and Parra-Rojas et al. (2015) had found an important production of $N_2O$ in sprites due to the chemical reaction $N_2 + O^- \rightarrow e + N_2O$ with the concentration of $O^-$ being previously increased, with respect to background values, due to the action of sprite streamers (Luque & Gordillo-Vázquez, 2012). According to Parra-Rojas et al. (2015), the production of NO and $N_2O$ could spread down to 50 km altitude (Parra-Rojas et al., 2015). In particular, the density enhancement of $N_2O$ molecules due to the streamer channel (scale of seconds) between 50 and 60 km altitudes could be up to 2 orders of magnitude above the background value. There are no global measurements nor estimations on the global chemical impact of sprites in the concentration of $N_2O$ in the mesosphere. However, modeling results by Gordillo-Vázquez (2008) and Parra-Rojas et al. (2015) suggest that sprites could contribute to the global concentration of $N_2O$ in the mesosphere, specially over middle and low latitudes where sprites are more frequent (Chen et al., 2008).

According to computational models of streamers, laboratory experiments, and optical measurements, sprites emit light predominantly in the first and second positive systems of the molecular neutral nitrogen (1PS $N_2$ and the 2PS $N_2$, or simply FPS and SPS), the first negative system of the molecular nitrogen ion ($N_2^+$-1NS or simply FNS), the Meinel band of the molecular nitrogen ion (Meinel $N_2^+$), and the Lyman-Birge-Hopfield (LBH) band of the molecular neutral nitrogen (e.g., Armstrong et al., 1998; Gordillo-Vázquez et al., 2018; Kanmae et al., 2007; Kuo et al., 2005b; Sato et al., 2015; Stenbaek-Nielsen et al., 2007). Some authors have proposed the use of the ratios FNS to SPS and FPS to SPS to estimate the peak electric field in air discharges (Adachi et al., 2006; Bonaventura et al., 2011; Celestin & Pasko, 2010; Hoder, 2016; Hoder et al., 2012; Kim et al., 2003; Kozlov et al., 2001; Kuo et al., 2005a, 2009, 2013; Liu et al., 2006; Morrill et al., 2002; Paris et al., 2004, 2005; Pasko, 2010; Pérez-Invernón et al., 2018; Shcherbakov & Sigmond, 2007; Šimek, 2014). Recently, Ihaddadene and Celestin (2017) proposed the measurement of the ratio of the SPS to the LBH band as a possible method to estimate the sprite streamer altitude from space-based photometers, such as the Atmosphere-Space Interactions Monitor (ASIM) (Chanrion et al., 2019; Neubert et al., 2019) and the Tool for the Analysis of RAdiations from lightNIngs and Sprites (TARANIS) (Lefeuvre et al., 2008). According for the spatial non-uniformity of streamers, Malagón-Romero et al. (2019) introduced two new methods to estimate the peak electric field in streamer heads.

Recently, Ono and Komuro (2019) validated the use of 2-D self-consistent streamer models to simulate the chemical influence of streamers in air. They compared the simulated enhancement of ozone produced by one streamer at atmospheric pressure with laser spectroscopy measurements. In this work we couple an extensive kinetic model of 131 species interacting through 952 chemical reactions with a 2-D self-consistent sprite streamer electrodynamical model. This 2-D approach allows us to self-consistently calculate the chemical influence of a single sprite streamer between the altitudes 68 and 75 km. The implemented vibrational and electronical kinetics of $N_2$ enable us to calculate the contribution of single sprite streamers to the photometers of ASIM and TARANIS. According to our results, optical emissions produced in the glow emerging in the streamer channel prevent the estimation of the sprite streamer head altitude from space-based photometers.

## 2. Streamer Model

To study the propagation of a sprite streamer and the latter evolution of the channel, we use a 2-D cylindrically symmetric model. We describe the time evolution of the electron density $n_e$ and ion densities $n_i$ with the drift-diffusion-reaction equations coupled to Poisson's equation as follows:

$$\frac{\partial n_e}{\partial t} = C_e + \nabla \cdot (n_e \mu_e \mathbf{E} + D_e \nabla n_e) + S_{ph}, \tag{1a}$$

$$\frac{\partial n_i}{\partial t} = C_i + S_{ph} \quad \delta_{O_2^+,i}, \tag{1b}$$

$$-\nabla \cdot \mathbf{E} = \nabla^2 \phi = -\sum_s \frac{q_s n_s}{\epsilon_0}, \tag{1c}$$

where the $i$ indexes the different types of ions, $\mu_e$ is the electron mobility, $D_e$ is the electron diffusion coefficient, $\mathbf{E}$ is the electric field, and $C_{e,i}$ are the net production of electrons and ions due to chemical reactions. In the present model we consider ions motionless over the short time scales (of a few milliseconds) that we study and therefore we neglect their mobility and diffusion. We use the local field approximation, and, consequently, transport coefficients are derived from the electron energy distribution function (EEDF) that only depends on the local electric field. The symbol $\delta$ is the Kronecker delta, and $S_{ph}$ is the photoionization term that only applies to electrons and $O_2^+$. As for Poisson's Equation 1c, $\phi$ is the electrostatic potential, the sum extends over all the charged species $s$, $q_s$ is the charge of the species $s$, with $s$ running over ions as well as electrons, and $\epsilon_0$ is the vacuum permittivity.

Finite volume methods coupled to hyperbolic methods are suitable to solve the set of Equations 1a and 1b. To solve these equations we have used CLAWPACK/PETCLAW (Alghamdi et al., 2011; Clawpack Development Team, 2017; LeVeque, 2002). PETCLAW is built upon PETSc (Balay et al., 2016b, 2016a) and allows us to split the simulation domain into different subdomains (problems) that can be solved in parallel. Poisson's equation is solved using the generalized minimal residual method and the geometric algebraic multigrid preconditioner, both from the PETSc numerical library.

We consider that the streamer is completely formed between altitudes 74.82 and 68 km, and we calculate its chemical influence and optical emissions in this range of altitudes. This approach allows us to ensure that the seed does not excessively influence our results.

### 2.1. Chemical Model

We use a modified version of the set of chemical reactions for halos and elves collected in the Appendix of Pérez-Invernón et al. (2016a), based on sprite and halo models developed by previous studies (Gordillo-Vázquez, 2008, 2010; Parra-Rojas et al., 2013, 2015). In addition, the chemical reactions of the 2-D model of streamers developed by Malagón-Romero and Luqoue (2018) are added to the model. As sprite streamers take place in the upper mesosphere where the concentration of water is negligible, we do not include chemical reactions involving water in our simulation. Vibrational chemistry of $CO_2$ is not considered in this study.

This vibrational and electronical chemical model allows us to calculate the temporal evolution of the density of $N_2(B^3\Pi_g, v = 0, ..., 6)$, $N_2(C^3\Pi_u, v = 0, ..., 4)$, and $N_2(a^1\Pi_g, v = 0, ..., 15)$. Therefore, we can calculate the temporal evolution of the contribution of single sprite streamers to ASIM photometers (PH1: $337 \pm 2.5$ nm from the SPS, PH2: 180–230 nm from the LBH band) sampling at 100 kHz (Chanrion et al., 2019; Neubert et al., 2019) and TARANIS photometers (PH1: $337 \pm 5$ nm from the SPS, PH2: 145–280 nm from the LBH band, PH3: 757–765 nm from the FPS, PH4: 600–800 nm from the FPS) sampling at 20 kHz (Lefeuvre et al., 2008).

We use the software QtPlaskin, developed by Luque (2011), to analyze the main chemical processes that contribute to the concentration of each chemical species as a function of time in our simulation.

### 2.2. Initial and Boundary Conditions

Sprites are high-altitude discharges made of many streamers that propagate through a varying air density. In our model, we have set as initial state of the atmosphere the chemical profiles of Figure 1 of Pérez-Invernón et al. (2018); that is, we set the air density profile and composition at nighttime conditions in November from the Whole Atmosphere Community Climate Model (WACCM) (Marsh et al., 2013) for a latitude of 38° and a longitude of 0° relaxed for 6.5 s under the presence of cosmic ray ionization (Thomas, 1974). The concentration of N is negligible, and the humidity is set to zero (dry air conditions). We also set a background electron density following the Wait-Spies profile (Hu et al., 2007) that is neutralized by an identical density of positive ions:

$$n_{e,bg} = \left(10^4 \text{ m}^{-3}\right) \times e^{-(z-60 \text{ km})/2.86 \text{ km}}. \tag{2}$$

In order to start the streamer we set a gaussian seed with an $e$-folding radius of 40 m and a peak density of $5 \times 10^{10}$ m$^{-3}$. This initial electron density is neutralized by an identical density of positive ions. In order to

solve Poisson's equation we impose Dirichlet boundary conditions at $z{=}z_{min}$ and free boundary conditions at $r{=}r_{max} = 600$ m and $z{=}z_{max}$ according to the method described by Malagón-Romero and Luqoue (2018). These free boundary conditions are consistent with the density charge inside the domain and with a potential decaying far away from the source.

We have simulated a positive streamer propagating in a background electric field of 100 V/m, which correspond to 120 Td at 74.23 km. The simulated domain extends from 67 to 75 km in the vertical direction, and the grid resolution is 1 m.

## 3. Results and Discussion

### 3.1. Chemical Influence of Sprite Streamers in the MLT

Figures 1a–1g show the most significant density enhancements of the selected chemical species produced in the central axis of a simulated streamer. The species production is integrated during 0.85 ms, a time in which the streamer tip advances from 74.82 to 67 km of altitude. Figure 1h shows the rates of production and losses of some species at 73 km of altitude. The streamer head reaches the altitude 73 km at time 0.45 ms. The density of the emitting species $N_2(C^3\Pi_u, v = 0)$ (Figure 1g) shows a glow emerging between $z = 74$ km and $z = 72$ km.

The main production of $N_2O$ takes place in the streamer channel region where the glow emerges (see Figure 1), while the densities of e, O, N, and NO are significantly perturbed in both the streamer head and the streamer channel. The obtained perturbation in the concentration of $O_3$ is 7 orders of magnitude lower than the background value (Pérez-Invernón et al., 2018). The high electric field in the head and channel of the streamer accelerates electrons, producing a high concentration of $O^-$, $N_2(A^3\Sigma_u^+)$, and other chemical species due to direct electron-impact ionization, excitation, and dissociation and electron detachment processes (Luque & Gordillo-Vázquez, 2012).

The main production mechanism of $N_2O$ is the electron detachment process $N_2 + O^- \rightarrow e + N_2O$. The production rate of $N_2O$ by the chemical process $N_2(A^3\Sigma_u^+, v = 0) + O_2 \rightarrow O + N_2O$ is 1 order of magnitude lower than the production of $N_2O$ by electron detachment. The most significant removal of $N_2O$ occurs in the streamer head, through ionization of $N_2O$ by electron impact, while the $N_2O$ losses in the streamer channel are dominated by the chemical reactions $e + N_2O \rightarrow N_2 + O^-$, $O^- + N_2O \rightarrow NO^- + NO$, and $N_2(A^3\Sigma_u^+, v = 0) + N_2O \rightarrow N_2 + N + NO$. We have obtained an increase in the concentration of $N_2O$ between 75 and 68 km during 0.85 ms 1 order of magnitude lower than the increase reported by Parra-Rojas et al. (2015) for 1 ms using a 0-D model.

The production of NO is dominated by the chemical reactions $O_2 + N(^2D) \rightarrow NO + O$ and $O_2 + N(^2P) \rightarrow NO + O$. Main losses of NO are due to ionization by electron impact in the streamer head and by the chemical reactions $NO + N(^2D) \rightarrow N_2 + O$ and $NO + N_2(A^3\Sigma_u^+, v = 0) \rightarrow N_2 + NO(A^2\Sigma^+)$ in the streamer channel. Processes involving $N_2^+$ and $O_2^+$ represent secondary mechanisms for the loss of NO.

Dvorak et al. (2019) recently measured in laboratory experiments a density enhancement of N inside the streamer channel. They proposed electron-ion dissociative recombination processes as the main mechanism producing an enhancement of N in the streamer channel. According to our results, the production of N by direct electron-impact dissociation of $N_2$ driven by the electric field in the streamer channel is 4 orders of magnitude above the production of N by electron-ion dissociative recombination processes. This apparent disagreement could be due to a lower importance of recombination processes at low density than at atmospheric conditions. In addition, the characteristic time of recombination processes is larger than the time simulated. The density of $O_3$ is reduced in the streamer channel due to the electron attachment process $e + O_3 \rightarrow O^- + O_2$. For a more detailed discussion of the main chemical mechanisms involved in this simulation, we refer to Parra-Rojas et al. (2015) and Pérez-Invernón et al. (2018).

In Figure 2 we show the vertically and horizontally integrated radial density enhancement of some chemical species produced by a simulated sprite streamer 0.85 ms after its onset. This figure shows for the first time the radial dependence of the production of NO and $N_2O$ by a sprite streamer. The production of chemical species in the simulated streamer decays radially around 2 orders of magnitude between the center of the streamer and 400 m. The production of N, NO, and electrons increases during the downward propagation of the streamer head. The maximum production of $N_2O$ takes place in the glow (above 72 km).

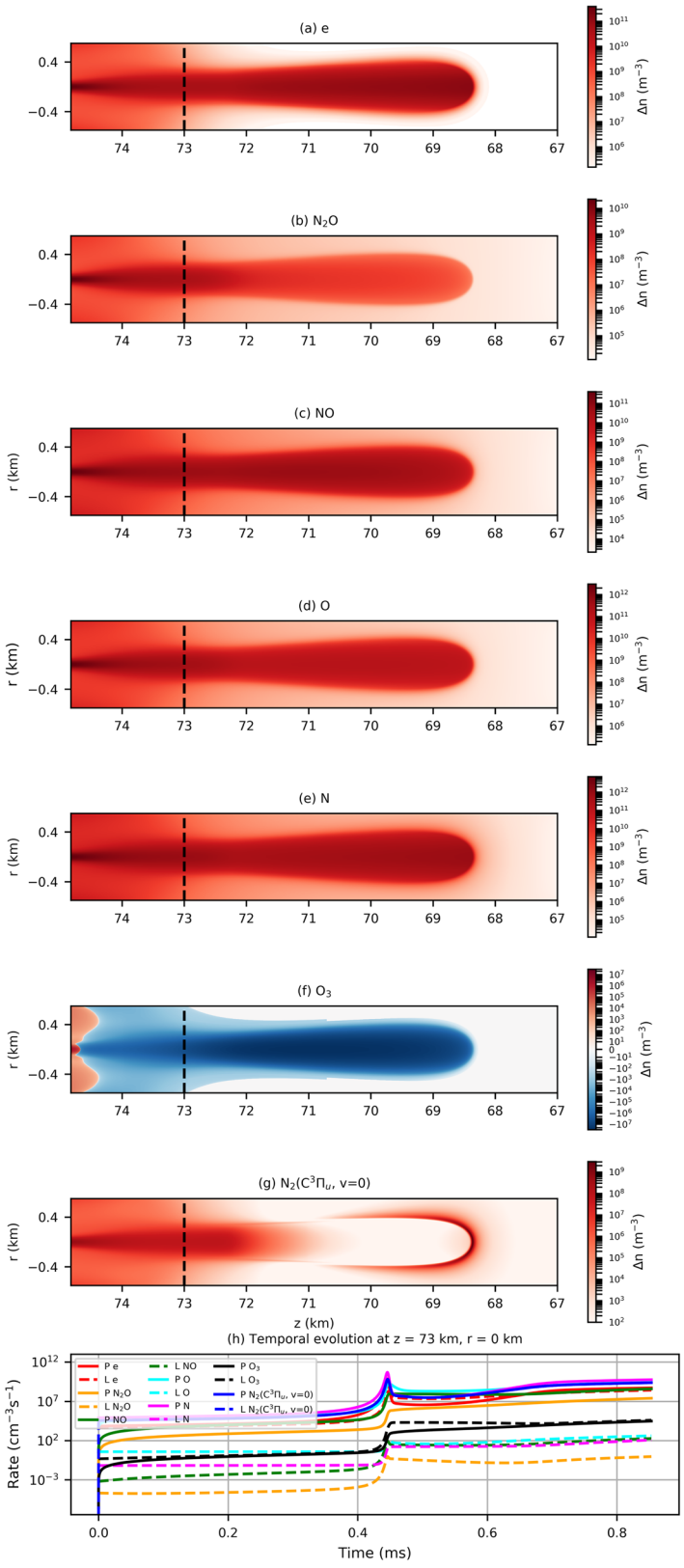


**Figure 1.** (a–g) Density enhancement with respect to background of different chemical species produced by a simulated sprite streamer 0.85 ms after its onset between altitudes 68 and 74.82 km. (h) Temporal evolution of the rates of production (P) and losses (L) of the species plotted in panels (a)–(f) at the position $z = 73$ km, $r = 0$ km.

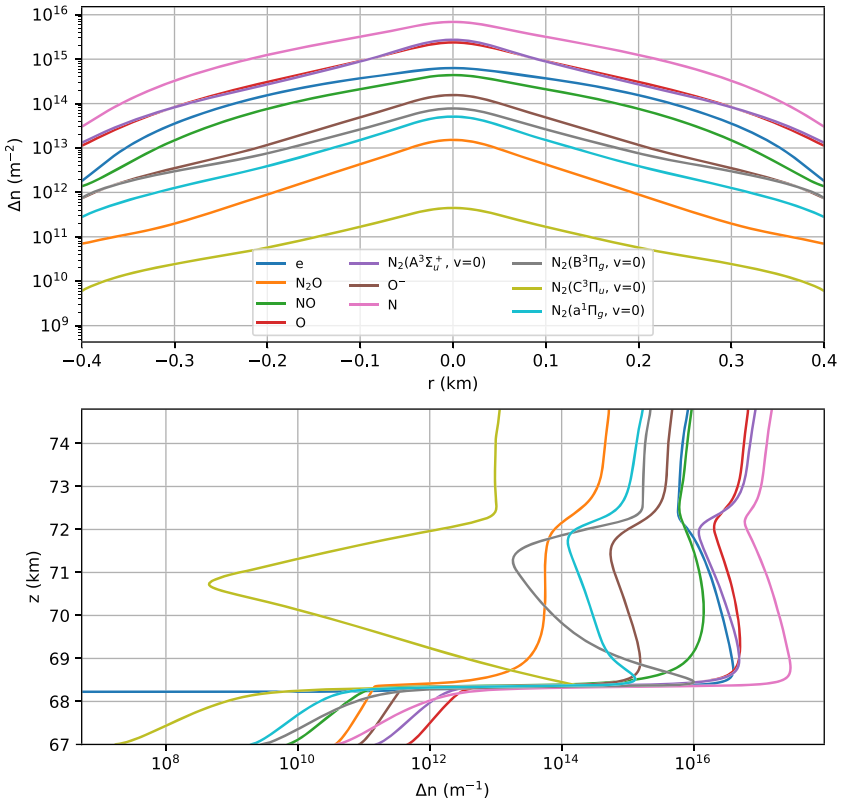


**Figure 2.** Vertically (upper panel) and horizontally (lower panel) integrated radial density enhancement of some chemical species produced by a simulated sprite streamer 0.85 ms after its onset between altitudes 68 and 74.82 km.

In Table 1 we show the most important productions of atoms and molecules in the mesosphere by a sprite streamer 0.85 ms after its onset in a cylindrical volume with a radius of 0.45 km and altitudes ranging from 67 up to 74.82 km. Computational limitations of this self-consistent electrodynamical model do not allow us to extend the simulation to longer times. We obtain streamer diameters of hundreds of meters, in agreement with previous observation (Cummer et al., 2006; Stenbaek-Nielsen et al., 2013) and modeling results (Luque & Ebert, 2009) of sprite streamers before bifurcation. We have obtained an injection of $5.9 \times 10^{19}$ NO molecules per sprite streamer, consistent with the production of $5 \times 10^{19}$ NO reported by Sentman et al. (2008) using a zero-dimensional model. The ratio of produced O atoms to NO molecules is about 5 in agreement with Sentman et al. (2008). According to our calculations, a sprite streamer could produce about $10^{18}$ $N_2O$ molecules between 68 and 74.82 km.

Let us now estimate the chemical influence of a sprite composed by several streamers in the MLT using measured optical signatures of sprites. Armstrong et al. (1998) reported the maximum brightness of a complete sprite to be about 150 kR using a ground-based photometer covering 6° of field of view (FOV), centered at 399.4 nm, and sampling at 750 Hz. The wavelength of the SPS that contributes to this photometer is 399.7 nm (Gilmore, 1992). The maximum brightness is reached in the first millisecond. In addition, Figure 5 of Armstrong et al. (1998) shows that the FOV of the photometer covers a significant part of the sprite. Therefore, we can compare the maximum brightness reported by these authors with the maximum brightness of the complete sprite in the total simulated time 0.85 ms. We use the density of $N_2(C^3\Pi_u,v)$ in our simulated single streamer, the atmospheric absorption calculated using the software MODTRANS 5 (Berk et al., 2005) between the sprite and the observer, and the system response of the photometer employed by Armstrong

**Table 1**
*Chemical Influence of the Simulated Sprite Streamer on the Concentration of Different Chemical Species Between 68 and 74.82 km*

| Species | Total number of produced atoms/molecules |
|---|---|
| N | $9.7 \times 10^{20}$ |
| O | $2.7 \times 10^{20}$ |
| NO | $5.9 \times 10^{19}$ |
| $N_2O$ | $1.2 \times 10^{18}$ |
| $O_3$ | $-1.8 \times 10^{16}$ |
| CO | $-3.1 \times 10^{15}$ |
| $CO_2$ | $3.1 \times 10^{15}$ |

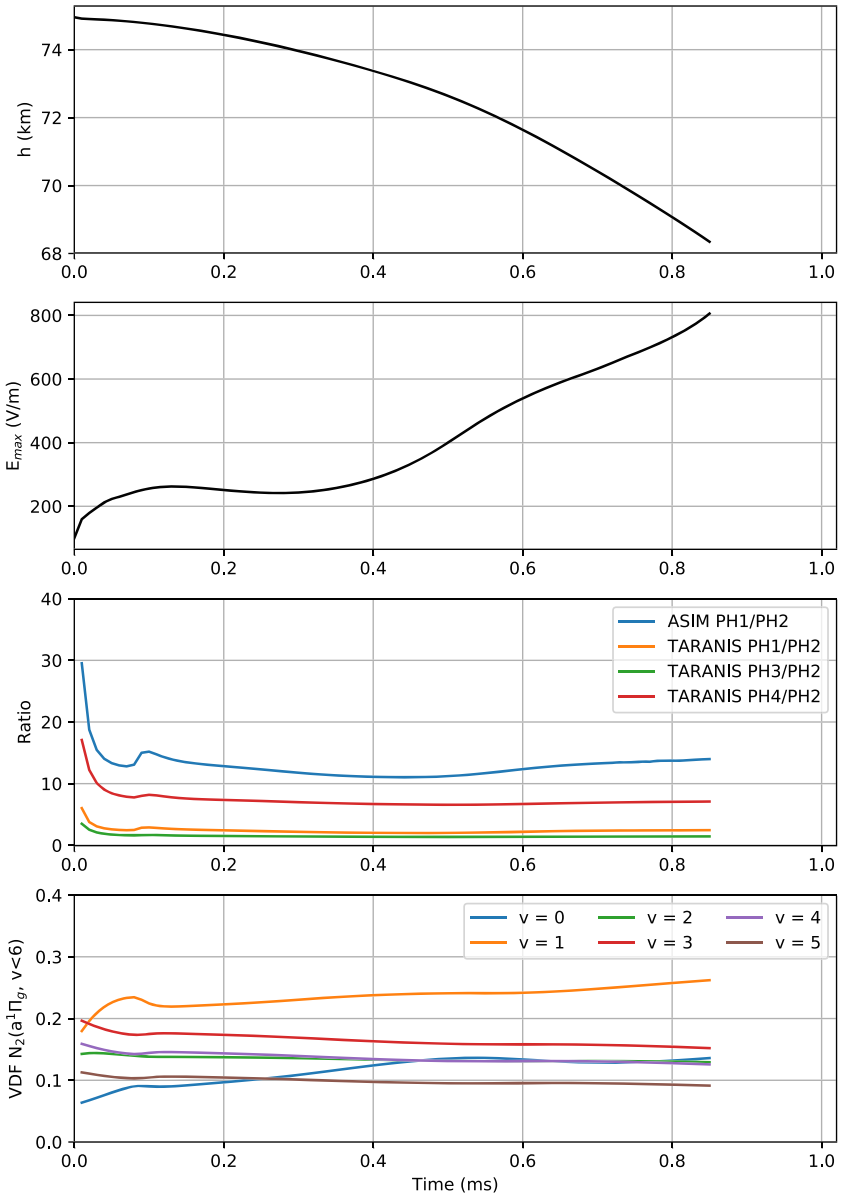


**Figure 3.** Temporal evolution of (a) the altitude of the streamer head, (b) the maximum electric field in the streamer head, (c) the ratio of the contributions of the simulated sprite streamer optical emissions to the photometers of ASIM (PH1: 337 ± 2.5 nm, PH2: 180–230 nm) and TARANIS (PH1: 337 ± 5 nm, PH2: 145–280 nm, PH3: 757–765 nm, PH4: 600–800 nm), and (d) the VDF of $N_2(a^1\Pi_g, v = 0, ..., 5)$.

et al. (1998) to estimate the optical signature, obtaining a maximum brightness of 3 kR. Therefore, the simulated brightness of a streamer is about 50 times less than the reported optical emissions of a complete sprite.

On the other hand, the Global Lightning and Sprite Measurements on Japanese Experiment Module (JEM-GLIMS) reported absolute peak intensity of a complete sprite of about $3 \times 10^{-6}$ W/m$^2$ with a photometer sampling at 20 kHz in a range of wavelengths between 150 and 280 nm at 410 km altitude (Sato et al., 2016). We use the density of $N_2(a^1\Pi_g, v)$ in our simulated streamer to estimate the optical signature in the photometer of JEM-GLIMS, obtaining a peak intensity of $1.6 \times 10^{-7}$ W/m$^2$. Therefore, we can assume that a complete sprite would produce between 18 and 50 times more optical emissions and production of chemical species than the simulated single streamer. We will use factor 18, which is calculated from space-based measurements that are not significantly influenced by the absorption of the atmosphere.

We have compared the maximum brightness of simulated and reported sprites in the first millisecond after their onset to estimate the production of chemical species by a complete sprite in about 1 ms. During this time, the streamers travel about 7 km downward. According to this comparison, a complete sprite would produce about $2 \times 10^{19}$ molecules of $N_2O$ and $10^{21}$ molecules of NO between about 68 and 75 km. Assuming a global sprite occurrence of 0.5 per minute (Chen et al., 2008), sprites could inject about $10^{25}$ $N_2O$ and $10^{27}$ NO molecules in the MLT annually. Since the average concentration of $N_2O$ in the MLT is about 1 ppbv (Kelly et al., 2018; Sheese et al., 2016), the total number of molecules of $N_2O$ contained between 68 and 75 km is about $3 \times 10^{30}$. Therefore, the injection of $N_2O$ molecules by sprites would contribute to the latitude-height profiles of $N_2O$ measured by ACE-FTS (Kelly et al., 2018; Sheese et al., 2016) by less than 0.003% of the total population per year for a sprite simulation up to 0.85 ms. Hence, the chemical effect of sprite seems to be not enough to explain the disagreement between the concentration of $N_2O$ in the MLT over middle and low latitudes measured by ACE-FTS (Sheese et al., 2016) and concentrations simulated by using WACCM4 (Kelly et al., 2018).

Our results correspond, however, to a simulation of 0.85 ms. The present computational capabilities do not allow more extensive spatiotemporal simulations with 2-D models. This means that we are only reporting the complete chemical influence of a sprite streamer head between altitudes 68 and 74.82 km and the influence of the first millisecond evolution of the streamer channel and the glow. The production of $N_2O$ and NO in the glow is still active at the end of the simulation. However, the 0-D simulation by Parra-Rojas et al. (2015) shows that the chemical influence of one sprite between 68 and 74.82 km altitudes would not significantly change between 0.85 ms and 100 s after the onset of the sprite streamer (see Figures 8 and 15 of Parra-Rojas et al., 2015).

### 3.2. Optical Signature From Space-Based Photometers

Our chemical model incorporates all mechanisms that influence the population of excited species that emit observable radiation. Figure 3 shows an analysis of the contribution of a simulated sprite streamer optical signature to the photometers of ASIM and TARANIS. We plot in the first and second panels of Figure 3 the altitude and maximum electric field of the downward propagating streamer head, respectively. The third panel of Figure 3 shows the ratio of the contributions of the simulated sprite streamer optical emissions to the different photometers of ASIM and TARANIS. Comparison of the three uppermost panels of Figure 3 shows that the photometer ratios do not provide information about the altitude of the streamer head. This is due to the significant contribution of the glow discharge to the total optical emissions of the sprite streamer. In addition, the temporal evolution of the vibrational distribution function (VDF) of the most populated vibrational states of $N_2(a^1\Pi_g, v)$ (Kirillov, 2011) showed in the fourth panel of Figure 3 is not constant during the temporal evolution of the simulated sprite streamer. The transient behavior of the $N_2(a^1\Pi_g, v)$ VDF is influenced by the radiative decay of the electronically excited $N_2(w^1\Delta_u, v)$ to $N_2(a^1\Pi_g, v = 0)$—with a characteristic time of 0.6 ms (Gilmore, 1992)—within the streamer channel. This cascading process breaks the assumption of a constant VDF of the $N_2(a^1\Pi_g, v)$ levels, which is required to calculate the contribution of the LBH into the photometer band and to estimate the altitude of the streamer head (Pérez-Invernón et al., 2018).

## 4. Summary and Conclusions

We have calculated the chemical influence and optical emissions of a sprite streamer at altitudes between 68 and 74.82 km and during 0.85 ms using a self-consistent 2-D model coupled with a kinetic scheme of 131 species interacting through 952 chemical reactions. Our results suggest that the injection of $N_2O$ by sprites in the MLT over midlatitudes and low latitudes is not enough to account for the disagreement between satellite observations and simulations. Future improvements in computational capabilities will allow more extensive spatiotemporal simulations to confirm this conclusion. The obtained injection of NO, N, and O molecules is in agreement with previous results based on 0-D and 1-D models. We have also estimated the contribution of the optical emissions of a simulated sprite streamer to the photometers of ASIM and TARANIS, concluding that the altitude of the streamer head cannot be estimated from space-based optical measurements operating at nadir.

The main conclusions of this work are as follows:

1. Single non-bifurcated sprite streamers can inject $9.7 \times 10^{20}$ atoms of N, $5.9 \times 10^{19}$ molecules of NO, and $1.2 \times 10^{18}$ molecules of $N_2O$ between the altitudes 68 and 74.82 km during 0.85 ms after its onset.
2. We have calculated for the first time the radial dependence of the production of NO and $N_2O$ by a single sprite streamer.
3. We have estimated the contribution of the sprite streamer optical signature to the ratio between optical signals recorded by different photometric recordings of ASIM and TARANIS.
4. According to our model, the LBH band optical emissions from the glow and the transient $N_2(a^1\Pi_g, v)$ VDF influenced by the radiative decay of $N_2(w^1\Delta_u, v)$ to $N_2(a^1\Pi_g, v = 0)$ prevent the estimation of the sprite streamer head altitude from space-based photometric recordings.

## Data Availability Statement

Data presented here are available at the IAA repository (https://cloud.iaa.csic.es/public.php?service=files&t=cb269d94561c81cdcdd5061f57cd86f0). The code developed for the simulation of sprite streamers is available at the repository (https://gitlab.com/amaro/streamer2d).

**Acknowledgments**

The authors acknowledge helpful discussions with Bernd Funke. This work was supported by the European Research Council (ERC) under the European Union H2020 program/ERC Grant Agreement 681257. This work has received funding from the Spanish Ministry of Economy and Competitiveness under Project ESP2017-86263-C4-4-R, from the Spanish Ministry of Science and Innovation (AEI) under Project PID2019-109269RB-C43, and from the FEDER program. F. J. P. I., A. M., and A. L. were supported by the European Research Council (ERC) under the European Union H2020 program/ERC Grant Agreement 68125. F. J. P. I. acknowledges the sponsorship provided by the Federal Ministry for Education and Research of Germany through the Alexander von Humboldt Foundation. Authors acknowledge financial support from the State Agency for Research of the Spanish MCIU through the "Center of Excellence Severo Ochoa" award for the Instituto de Astrofísica de Andalucía (SEV-2017-0709).

## References

Adachi, T., Fukunishi, H., Takahashi, Y., Hiraki, Y. H., Hsu, R.-R., Su, H.-T., et al. (2006). Electric field transition between the diffuse and streamer regions of sprites estimated from ISUAL/array photometer measurements. *Geophysical Research Letters*, *33*, L17803. https://doi.org/10.1029/2006GL026495

Alghamdi, A., Ahmadia, A., Ketcheson, D. I., Knepley, M. G., Mandli, K. T., & Dalcin, L. (2011). PetClaw: A scalable parallel nonlinear wave propagation solver for Python, *Proceedings of the 19th High Performance Computing Symposia* (pp. 96–103). San Diego, CA, USA: Society for Computer Simulation International.

Armstrong, R. A., Shorter, J. A., Taylor, M. J., Suszcynsky, D. M., Lyons, W. A., & Jeong, L. S. (1998). Photometric measurements in the SPRITES 1995 and 1996 campaigns of nitrogen second positive (399.8 nm) and first negative (427.8 nm) emissions. *Journal of Atmospheric and Solar-Terrestrial Physics*, *60*, 787. https://doi.org/10.1016/S1364-6826(98)00026-1

Arnone, E., & Dinelli, B. M. (2016). CHIMTEA—Chemical impact of thunderstorms on Earth's atmosphere. In D. Fernández-Prieto & R. Sabia (Eds.), *Remote Sensing Advances for Earth System Science*, *Springer Earth System Sciences* (pp. 1–14). Cham: Springer.

Arnone, E. K., Kero, A., Dinelli, B. M., Enell, C.-F., & Arnold, N. F. (2009). Seeking sprite-induced signatures in remotely sensedmiddle atmosphere $NO_2$: Latitude and time variations. *Plasma Sources Science and Technology*, *18*(3), 34,014. https://doi.org/10.1088/0963-0252/18/3/034014

Arnone, E. K., Kero, A., Dinelli, B. M., Enell, C.-F., Arnold, N. F., Papandrea, E., et al. (2008). Seeking sprite-induced signatures in remotely sensed middle atmosphere $NO_2$. *Geophysical Research Letters*, *35*, L05807. https://doi.org/10.1029/2007GL031791

Arnone, E. S., Smith, A. K., Enell, C.-F., Kero, A., & Dinelli, B. M. (2014). WACCM climate chemistry sensitivity to sprite perturbations. *Journal of Geophysical Research: Atmospheres*, *119*, 6958–6970. https://doi.org/10.1002/2013JD020825

Balay, S., Abhyankar, S., Adams, M. F., Brown, J., Brune, P., Buschelman, K., & Zhang, H. (2016a). *PETSc users manual* (*ANL-95/11 - Revision 3.7*). Argonne National Laboratory. Retrieved from https://www.mcs.anl.gov/petsc

Balay, S., Abhyankar, S., Adams, M. F., Brown, J., Brune, P., Buschelman, K., & Zhang, H. (2016b). *PETSc web page*. Retrieved from https://www.mcs.anl.gov/petsc

Berk, A., Anderson, G. P., Acharya, P. K., Bernstein, L. S., Muratov, L., & Lee, J. (2005). MODTRAN 5: A reformulated atmospheric band model with auxiliary species and practical multiple scattering options: Update. In *Algorithms and technologies for multispectral, hyperspectral, and ultraspectral imagery XI* (Vol. 5806, pp. 662–668). Orlando, FL: Society of Photo-Optical Instrumentation Engineers.

Bonaventura, Z. B., Bourdon, A., Celestin, S., & Pasko, V. P. (2011). Electric field determination in streamer discharges in air at atmospheric pressure. *Plasma Sources Science and Technology*, *20*, 35012. https://doi.org/10.1088/0963-0252/20/3/035012

Celestin, S., & Pasko, V. P. (2010). Effects of spatial non-uniformity of streamer discharges on spectroscopic diagnostics of peak electric fields in transient luminous events. *Geophysical Research Letters*, *37*, L07804. https://doi.org/10.1029/2010GL042675

Chanrion, O., Neubert, T., Rasmussen, I. L., Stoltze, C., Tcherniak, D., Jessen, N. C., et al. (2019). The Modular Multispectral Imaging Array (MMIA) of the ASIM payload on the International Space Station. *Space Science Reviews*, *215*(4), 28. https://doi.org/10.1007/s11214-019-0593-y

Chen, A. B., Kuo, C.-L., Lee, Y.-J., Su, H.-T., Hsu, R.-R., Chern, J.-L., et al. (2008). Global distributions and occurrence rates of transient luminous events. *Journal of Geophysical Research*, *113*, A08306. https://doi.org/10.1029/2008JA013101

Clawpack Development Team (2017). Clawpack software. Retrieved from http://www.clawpack.org (Version 5.4.1). https://doi.org/10.5281/zenodo.820730

Crutzen, P. J. (1979). The role of NO and $NO_2$ in the chemistry of the troposphere and stratosphere. *Annual review of earth and planetary sciences*, *7*(1), 443–472.

Cummer, S. A., Jaugey, N., Li, J., Lyons, W. A., Nelson, T. E., & Gerken, E. A. (2006). Submillisecond imaging of sprite development and structure. *Geophysical Research Letters*, *33*, L04104. https://doi.org/10.1029/2005GL024969

Davidson, E. A. (2009). The contribution of manure and fertilizer nitrogen to atmospheric nitrous oxide since 1860. *Nature Geoscience*, *2*(9), 659. https://doi.org/10.1038/ngeo608

Dvorak, P., Šimek, M., & Prukner, V. (2019). Evolution of N (4S) atoms produced under nitrogen streamer conditions: Time-resolved TALIF study at reduced pressures. *Plasma Sources Science and Technology*, *28*, 125004. https://doi.org/10.1088/1361-6595/ab36a5

Enell, C.-F., Arnone, E., Adachi, T., Chanrion, O., Verronen, P. T., Seppälä, A., & Hsu, R. R. (2008). Parameterisation of the chemical effect of sprites in the middle atmosphere. *Annales Geophysicae*, *26*, 13. https://doi.org/10.5194/angeo-26-13-2008

Evtushenko, A. A., Kuterin, F. A., & Mareev, E. A. (2013). A model of sprite influence on the chemical balance of mesosphere. *Journal of Atmospheric and Terrestrial Physics*, *102*, 298–310. https://doi.org/10.1016/j.jastp.2013.06.005

Franz, R. C., Nemzek, R. J., & Winckler, J. R. (1990). Television image of a large upward electrical discharge above a thunderstorm system. *Science*, *249*, 48. https://doi.org/10.1126/science.249.4964.48

Gilmore, F. R. L., P. J. (1992). Franck-Condon factors, r-centroids, electronic transition moments, and Einstein coefficients for many nitrogen and oxygen band systems. *Journal of Physical and Chemical Reference Data*, *21*, 1005. https://doi.org/10.1063/1.555910

Gordillo-Vázquez, F. J. (2008). Air plasma kinetics under the influence of sprites. *Journal of Physics D: Applied Physics*, *41*(23), 234,016. https://doi.org/10.1088/0022-3727/41/23/234016

Gordillo-Vázquez, F. J. (2010). Vibrational kinetics of air plasmas induced by sprites. *Journal of Geophysical Research*, *115*, A00E25. https://doi.org/10.1029/2009JA014688

Gordillo-Vázquez, F. J., Luque, A., & Simek, M. (2012). Near infrared and ultraviolet spectra of TLEs. *Journal of Geophysical Research*, *117*, A05329. https://doi.org/10.1029/2012JA017516

Gordillo-Vázquez, F. J., Passas, M., Luque, A., Saánchez, J., Velde, O. A., & Montanyá, J. (2018). High spectral resolution spectroscopy of sprites: A natural probe of the mesosphere. *Journal of Geophysical Research: Atmospheres*, *123*, 2336–2346. https://doi.org/10.1002/2017JD028126

Hoder, T. S., F. J. (2016). Radially and temporally resolved electric field of positive streamers in air and modelling of the induced plasma chemistry. *Plasma Sources Science and Technology*, *25*, 45021. https://doi.org/10.1088/0963-0252/25/4/045021

Hoder, T., Černák, M., Paillol, J., Loffhagen, D., & Brandenburg, R. (2012). High-resolution measurements of the electric field at the streamer arrival to the cathode: A unification of the streamer-initiated gas-breakdown mechanism. *Physical Review E*, *86*(5), 55401. https://doi.org/10.1103/PhysRevE.86.055401

Hu, W., Cummer, S. A., & Lyons, W. A. (2007). Testing sprite initiation theory using lightning measurements and modeled electromagnetic fields. *Journal of Geophysical Research*, *112*, D13115. https://doi.org/10.1029/2006JD007939

Ihaddadene, M. A., & Celestin, S. (2017). Determination of sprite streamers altitude based on $N_2$ spectroscopic analysis. *Journal of Geophysical Research: Space Physics*, *122*, 1000–1014. https://doi.org/10.1002/2016JA023111

Kanmae, T., Stenbaek-Nielsen, H. C., & McHarg, M. G. (2007). Altitude resolved sprite spectra with 3 ms temporal resolution. *Geophysical Research Letters*, *34*, L07810. https://doi.org/10.1029/2006GL028608

Kelly, C., Chipperfield, M., Plane, J., Feng, W, Sheese, P, Walker, K. A., & Boone, C. D. (2018). An explanation for the nitrous oxide layer observed in the mesopause region. *Geophysical Research Letters*, *45*, 7818–7827. https://doi.org/10.1029/2018GL078895

Kim, Y., Hong, S. H., Cha, M. S., Song, Y. H., & Kim, S. J. (2003). Measurements of electron energy by emission spectroscopy in pulsed corona and dielectric barrier discharges. *Journal of Advanced Oxidation Technologies*, *6*(1), 17–22. https://doi.org/10.1515/jaots-2003-0103

Kirillov, A. S. (2011). Singlet molecular nitrogen in the Auroral ionosphere and under the conditions of laboratory discharge. *Technical Physics*, *56*(12), 1737–1744. https://doi.org/10.1134/s1063784211120085

Kozlov, K., Wagner, H., Brandenburg, R., & Michel, P. (2001). Spatio-temporally resolved spectroscopic diagnostics of the barrier discharge in air at atmospheric pressure. *Journal of Physics D: Applied Physics*, *34*(21), 3164. https://doi.org/10.1088/0022-3727/34/21/309

Kuo, C. L., Chou, J., Tsai, L., Chen, A., Su, H. T., Hsu, R. R., et al. (2009). Discharge processes, electric field, and electron energy in ISUAL-recorded gigantic jets. *Journal of Geophysical Research*, *114*, A04314. https://doi.org/10.1029/2008JA013791

Kuo, C. L., Hsu, R. R., Chen, A. B., Su, H. T., Lee, L. C., Mende, S. B., et al. (2005b). Electric fields and electron energies inferred from the ISUAL recorded sprites. *Geophysical Research Letters*, *32*, L19103. https://doi.org/10.1029/2005GL023389

Kuo, C. L., Hsu, R., Chen, A., Su, H., Lee, L. C., Mende, S., & Takahashi, Y. (2005a). Electric fields and electron energies inferred from the ISUAL recorded sprites. *Geophysical research letters*, *32*, 19. https://doi.org/10.1029/2005GL023389

Kuo, C. L., Williams, E., Bór, J., Lin, Y. H., Lee, L. J., Huang, S. M., et al. (2013). Ionization emissions associated with $N_2^+$ 1N band in halos without visible sprite streamers. *Journal of Geophysical Research*, *118*, 5317–5326. https://doi.org/10.1002/jgra.50470

LeVeque, R. J. (2002). *Finite volume methods for hyperbolic problems* (Vol. 31). Cambridge: Cambridge University Press.

Lefeuvre, F. B., Blanc, E., Pincon, J.-L., Roussel-Dupré, R., Lawrence, D., & Lagoutte, D. (2008). TARANIS—A satellite project dedicated to the physics of TLEs and TGFs. *Space Science Reviews*, *137*(1-4), 301–315. https://doi.org/10.1007/s11214-008-9414-4

Liu, N. (2010). Model of sprite luminous trail caused by increasing streamer current. *Geophysical Research Letters*, *37*, L04102. https://doi.org/10.1029/2009GL042214

Liu, N., Pasko, V. P., Burkhardt, D. H., Frey, H. U., Mende, S. B., Su, H.-T., et al. (2006). Comparison of results from sprite streamer modeling with spectrophotometric measurements by ISUAL instrument on FORMOSAT-2 satellite. *Geophysical Research Letters*, *33*, L01101. https://doi.org/10.1029/2005GL024243

Luque, A. (2011). Computer code QTPlaskin. Retrieved from https://github.com/aluque/qtplaskin

Luque, A., & Ebert, U. (2009). Emergence of sprite streamers from screening-ionization waves in the lower ionosphere. *Nature Geoscience*, *2*, 757–760.

Luque, A., & Gordillo-Vázquez, F. (2010). *Modeling of sprite beads: Using numerical streamer simulations to infer the pre-existing electron density in a sprite discharge*. Paper presented at AGU Fall Meeting Abstracts B3+.

Luque, A., & Gordillo-Vázquez, F. J. (2011). Sprite beads originating from inhomogeneities in the mesospheric electron density. *Geophysical Research Letters*, *38*, L04808. https://doi.org/10.1029/2010GL046403

Luque, A., & Gordillo-Vázquez, F. J. (2012). Mesospheric electric breakdown and delayed sprite ignition caused by electron detachment. *Nature Geoscience*, *4*, 22–25. https://doi.org/10.1038/ngeo1314

Luque, A., Stenbaek-Nielsen, H., McHarg, M., & Haaland, R. (2016). Sprite beads and glows arising from the attachment instability in streamer channels. *Journal of Geophysical Research: Space Physics*, *121*, 2431–2449. https://doi.org/10.1002/2015JA022234

Malagón-Romero, A., & Luqoue, A. (2018). A domain-decomposition method to implement electrostatic free boundary conditions in the radial direction for electric discharges. *Computer Physics Communications*, *225*(14), 114–121. https://doi.org/10.1016/j.cpc.2018.01.003

Malagón-Romero, A., Pérez-Invernón, F., Luque, A., & Gordillo-Vázquez, F. (2019). Analysis of the spatial non-uniformity of the electric field in spectroscopic diagnostic methods of atmospheric electricity phenomena. *Journal of Geophysical Research: Atmospheres*, *124*, 12,356–12,370. https://doi.org/10.1029/2019JD030945

Marsh, D. R., Mills, M. J., Kinnison, D. E., Lamarque, J. F., Calvo, N., & Polvani, L. M. (2013). Climate change from 1850 to 2005 simulated in CESM1 (WACCM). *Journal of Climate*, *26*(19), 7372–7391. https://doi.org/10.1175/JCLI-D-12-00558.1

Morrill, J., Bucsela, E., Siefring, C., Heavner, M., Berg, S., Moudry, D., & Osborne, D. (2002). Electron energy and electric field estimates in sprites derived from ionized and neutral $N_2$ emissions. *Geophysical Research Letters*, *29*(10), 1462. https://doi.org/10.1029/2001GL014018

Neubert, T., Østgaard, N., Reglero, V., Blanc, E., Chanrion, O., Oxborrow, C. A., & Bhanderi, D. D. (2019). The ASIM mission on the International Space Station. *Space Science Reviews*, *215*(2), 26. https://doi.org/10.1007/s11214-019-0592-z

Ono, R., & Komuro, A. (2019). Generation of the single-filament pulsed positive streamer discharge in atmospheric-pressure air and its comparison with two-dimensional simulation. *Journal of Physics D: Applied Physics*, *53*(3), 35,202. https://doi.org/10.1088/1361-6463/ab4e65

Paris, P., Aints, M., Laan, M., & Valk, F. (2004). Measurement of intensity ratio of nitrogen bands as a function of field strength. *Journal of Physics D: Applied Physics*, *37*(8), 1179. https://doi.org/10.1088/0022-3727/37/8/005

Paris, P., Aints, M., Valk, F., Plank, T., Haljaste, A., Kozlov, K. V., & Wagner, H.-E. (2005). Intensity ratio of spectral bands of nitrogen as a measure of electric field strength in plasmas. *Journal of Physics D: Applied Physics*, *38*, 3894. https://doi.org/10.1088/0022-3727/38/21/010

Parra-Rojas, F. C., Luque, A., & Gordillo-Vázquez, F. J. (2013). Chemical and electrical impact of lightning on the Earth mesosphere: The case of sprite halos. *Journal of Geophysical Research: Atmospheres*, *118*, 5190–5214. https://doi.org/10.1002/jgra.50449

Parra-Rojas, F. C., Luque, A., & Gordillo-Vázquez, F. J. (2015). Chemical and thermal impact of sprite streamers in the Earth mesosphere. *Journal of Geophysical Research: Space Physics*, *120*, 8899–8933. https://doi.org/10.1002/2014JA020933

Pasko, V. P. (2010). Recent advances in theory of transient luminous events. *Journal of Geophysical Research*, *115*, A00E35. https://doi.org/10.1029/2009JA014860

Pasko, V. P., Inan, U. S., & Bell, T. F. (1998). Spatial structure of sprites. *Geophysical Research Letters*, *25*, 2123. https://doi.org/10.1029/98GL01242

Pasko, V. P., Inan, U. S., Bell, T. F., & Taranenko, Y. N. (1997). Sprites produced by quasi-electrostatic heating and ionization in the lower ionosphere. *Journal of Geophysical Research*, *102*, 4529. https://doi.org/10.1029/96JA03528

Pasko, V. P., Yair, Y., & Kuo, C.-L. (2012). Lightning related transient luminous events at high altitude in the Earth's atmosphere: Phenomenology, mechanisms and effects. *Space Science Reviews*, *168*, 475–516. https://doi.org/10.1007/s11214-011-9813-9

Pérez-Invernón, F. J., Gordillo-Vázquez, F. J., Smith, A. K., Arnone, E., & Winkler, H. (2019). Global occurrence and chemical impact of stratospheric Blue Jets modeled with WACCM4. *Journal of Geophysical Research: Atmospheres*, *124*, 2841–2864. https://doi.org/10.1029/2018JD029593

Pérez-Invernón, F. J., Luque, A., & Gordillo-Vázquez, F. J. (2018). Modeling the chemical impact and the optical emissions produced by lightning-induced electromagnetic fields in the upper atmosphere: The case of halos and elves triggered by different lightning discharges. *Journal of Geophysical Research: Atmospheres*, *123*, 7615–7641. https://doi.org/10.1029/2017JD028235

Pérez-Invernón, F. J., Luque, A., Gordillo-Vazquez, F. J., Sato, M., Ushio, T., Adachi, T., & Chen, A. B. (2018). Spectroscopic diagnostic of halos and elves detected from space-based photometers. *Journal of Geophysical Research: Atmospheres*, *123*, 12,917–12,941. https://doi.org/10.1029/2018JD029053

Raizer, Y. P., Milikh, G. M., Shneider, M. N., & Novakovski, S. V. (1998). Long streamers in the upper atmosphere above thundercloud. *Journal of Physics D: Applied Physics*, *31*, 3255. https://doi.org/10.1088/0022-3727/31/22/014

Rodger, C. J., Seppää, A., & Clilverd, M. A. (2008). Significance of transient luminous events to neutral chemistry: Experimental measurements. *Geophysical Research Letters*, *35*, L07803. https://doi.org/10.1029/2008GL033221

Sato, M., Mihara, M., Adachi, T., Ushio, T., Morimoto, T, Kikuchi, M., et al. (2016). Horizontal distributions of sprites derived from the JEM-GLIMS nadir observations. *Journal of Geophysical Research: Atmospheres*, *121*, 3171–3194. https://doi.org/10.1002/2015JD024311

Sato, M., Ushio, T., Morimoto, T, Kikuchi, M, Kikuchi, H, Adachi, T., et al. (2015). Overview and early results of the Global Lightning and Sprite Measurements mission. *Journal of Geophysical Research: Atmospheres*, *120*, 3822–3851. https://doi.org/10.1002/2014JD022428

Schumann, U., & Huntrieser, H. (2007). The global lightning-induced nitrogen oxides source. *Atmospheric Chemistry and Physics*, *7*, 823. https://doi.org/10.5194/acp-7-3823-2007

Sentman, D. D., Stenbaek-Nielsen, C., McHarg, M. G., & Morrill, J. S. (2008). Plasma chemistry of sprite streamers. *Journal of Geophysical Research*, *113*, D11112. https://doi.org/10.1029/2007JD008941

Shcherbakov, Y. V., & Sigmond, R. (2007). Subnanosecond spectral diagnostics of streamer discharges: I. Basic experimental results. *Journal of Physics D: Applied Physics*, *40*(2), 460. https://doi.org/10.1088/0022-3727/40/2/023

Sheese, P. E, Walker, K. A, Boone, C. D, Bernath, P. F., & Funke, B. (2016). Nitrous oxide in the atmosphere: First measurements of a lower thermospheric source. *Geophysical Research Letters*, *43*, 2866–2872. https://doi.org/10.1002/2015GL067353

Stenbaek-Nielsen, H. C., Kanmae, T., & McHarg, M. G. (2013). High-speed observations of sprite streamers. *Surveys in Geophysics*, *34*, 769. https://doi.org/10.1007/s10712-013-9224-4

Stenbaek-Nielsen, H. C., McHarg, M. G., Kanmae, T., & Sentman, D. D. (2007). Observed emission rates in sprite streamer heads. *Geophysical Research Letters*, *34*, L11105. https://doi.org/10.1029/2007GL029881

Stenbaek-Nielsen, H. C., Moudry, D. R., Wescott, E. M., Sentman, D. D., & Sao Sabbas, F. T. (3829). Sprites and possible mesospheric effects. *Geophysical Research Letters*, *27*. https://doi.org/10.1029/2000GL003827

Thomas, L. (1974). Recent developments and outstanding problems in the theory of the D region. *Radio Science*, *9*(2), 121. https://doi.org/10.1029/RS009i002p00121

Winkler, H., & Nothold, J. (2014). The chemistry of daytime sprite streamers—A model study. *Atmospheric Chemistry and Physics*, *14*, 3545–3556. https://doi.org/10.5194/acp-14-3545-2014

Winkler, H., & Nothold, J. (2015). A model study of the plasma chemistry of stratospheric Blue Jets. *Journal of Atmospheric and Solar-Terrestrial Physics*, *122*, 75. https://doi.org/10.1016/j.jastp.2014.10.015

Šimek, M. (2014). Optical diagnostics of streamer discharges in atmospheric gases. *Journal of Physics D: Applied Physics*, *47*(46), 463,001. https://doi.org/10.1088/0022-3727/47/46/463001